We are IntechOpen, the world's leading publisher of Open Access books
Built by scientists, for scientists

4,800
Open access books available

122,000
International authors and editors

135M
Downloads

Our authors are among the

154
Countries delivered to

TOP 1%
most cited scientists

12.2%
Contributors from top 500 universities

CLARIVATE ANALYTICS
BOOK CITATION INDEX
INDEXED

WEB OF SCIENCE™

Selection of our books indexed in the Book Citation Index in Web of Science™ Core Collection (BKCI)

Interested in publishing with us?
Contact book.department@intechopen.com

Numbers displayed above are based on latest data collected.
For more information visit www.intechopen.com

Chapter 9

Evaluation of Adaptive Bone Remodeling after Total Hip Arthroplasty Using Finite Element Analysis

Yutaka Inaba, Hiroyuki Ike, Masatoshi Oba and Tomoyuki Saito

Additional information is available at the end of the chapter

http://dx.doi.org/10.5772/65031

Abstract

We compared equivalent stress and strain energy density (SED) to bone mineral density (BMD) in the femur after total hip arthroplasty (THA) using subject-specific finite element analysis (FEA). Equivalent stress and BMD were maintained in the distal femur after THA, whereas both decreased in the proximal femur. A significant correlation was observed between the rates of changes in BMD and equivalent stress before and after THA. Therefore, FEA can predict adaptive bone remodeling after mechanical loading changes. Additionally, we evaluated the effects of two different types of stem geometries (Zweymüller-type stem and fit-and-fill-type stem) on load distribution and BMD using the same method. Equivalent stress and BMD in the medial side of the proximal femur were significantly lower with the Zweymüller-type stem than with the fit-and-fill-type stem. Therefore, FEA can assess the effects of stem geometry on bone remodeling after THA. Moreover, we evaluated the effects of bone geometry on load distribution and BMD after THA. Equivalent stress in the medial side of the proximal femur was significantly lower in the stovepipe model implanted with large tapered wedge-type stems than in the champagne flute and intermediate models, and there was a significant loss of BMD in the stovepipe model. Therefore, a large tapered wedge-type stem and stovepipe femur may be associated with significant proximal BMD loss.

Keywords: finite element analysis, dual-energy X-ray absorptiometry, bone remodeling, hip, arthroplasty

INTECH
open science | open minds

© 2017 The Author(s). Licensee InTech. This chapter is distributed under the terms of the Creative Commons Attribution License (http://creativecommons.org/licenses/by/3.0), which permits unrestricted use, distribution, and reproduction in any medium, provided the original work is properly cited. CC BY

1. Introduction

Periprosthetic bone loss, i.e., a decrease in bone mineral density (BMD) around an implant, is a major concern following total hip arthroplasty (THA) [1, 2]. Severe periprosthetic bone loss may contribute to aseptic loosening of the prosthesis or the risk of periprosthetic fracture [3] and presents serious problems if revision surgery becomes necessary [4]. Several studies have reported that BMD decreases following THA, particularly in the proximal femur [5, 6]. Most changes in BMD occur during the first postoperative year, and subsequently, BMD is maintained [7–9]. This phenomenon is considered to be an adaptive remodeling response of the bone structure to alter its stress environment owing to the presence of an implant. Therefore, mechanical stress may be associated with the patterns of BMD changes. In particular, in cementless THA, an optimal fit of the stem into the metaphyseal region of the femur has been reported to lead to a reduction in periprosthetic bone loss [10].

Wolff [11] proposed that trabecular bone in the proximal femur adapts to external mechanical loads. This structural change is caused by bone remodeling, which couples bone resorption by osteoclasts and bone formation by osteoblasts [12]. It is generally accepted that bone tissue can detect and respond to its mechanical environment, but the exact mechanical signal that drives remodeling remains controversial [13]. Various biomechanical parameters have been investigated to determine the remodeling stimulus. Huiskes et al. [14] examined whether strain energy density (SED) controls bone remodeling. Carter et al. [15] examined stress, and Stulpner et al. [16] examined equivalent strain as signals for remodeling. Adachi et al. [17] proposed that the driving force of remodeling is the local nonuniformity of the scalar function of stress. The existence of various theories indicates that the mechanism of bone remodeling is not well understood.

Subject-specific finite element (FE) models based on geometry and mechanical properties derived from computed tomography (CT) scans have been described in several studies [18–20]. Furthermore, relationships between results of subject-specific finite element analysis (FEA) and bone density have been investigated previously. Cody et al. [21] performed subject-specific FEA and bone density measurements for predicting the fracture load of the femur. Tawara et al. [22] evaluated vertebral strength using subject-specific FEA and BMD. We previously examined the usefulness of subject-specific FEA, which was validated by BMD changes, after THA. We found that equivalent stress through subject-specific FEA correlated with BMD changes before and after THA [23]. The distribution of mechanical loads within the femur after THA might be influenced by the stem geometry and the femur structure. Our previous results suggest that subject-specific FEA could be used to evaluate the effects of stem and femoral geometry on adaptive bone remodeling after THA [24].

This chapter initially provides general information on subject-specific FEA and then presents a brief overview of our work regarding adaptive bone remodeling after THA.

http://dx.doi.org/10.5772/65031

2. Finite element analysis

2.1. Finite element analysis and bone mineral density

It is difficult to assess the stress and strain distributions throughout the entire bone using simplified mathematical models or implanted prostheses or through experiments with cadaveric tissue. An alternative approach to analyze bone mechanics is the FE method, which can accommodate large intersubject variations in bone geometry and material properties [25]. When the ability to perform three-dimensional FE contact analysis is available, subject-specific geometry should be analyzed. This provides the opportunity to examine normal populations of individuals and populations with specific injuries or other pathologies. Ultimately, patient-specific modeling might be used in surgical planning and large-scale studies of treatment efficacy [26]. As mentioned above, we investigated the relationships between the FEA results and BMD. Several previous studies have described the application of FEA for investigating bone-remodeling patterns around implants. However, most of these were not subject-specific models. Weinans et al. [27] reported that subject-specific FE models might be useful for explaining variations in bone adaptation responsiveness among different subjects.

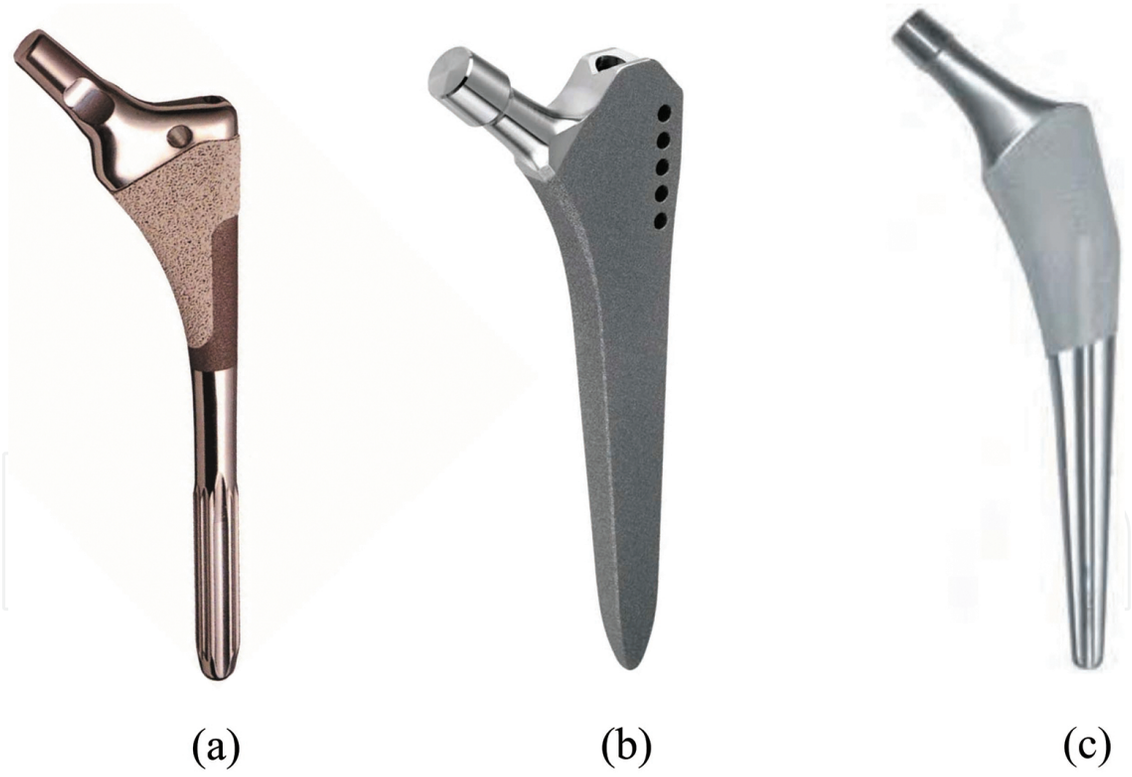

Figure 1. Diagrams of (a) collarless VerSys Fiber Metal MidCoat, (b) SL-PLUS, and (c) Accolade TMZF stems. (a) Collarless VerSys Fiber Metal MidCoat (Zimmer Inc., Warsaw, IN) is a fit-and-fill-type stem composed of titanium alloy with fiber-metal porous coating at the proximal region. (b) SL-PLUS (Smith & Nephew Inc., Memphis, TN) is a Zweymüller-type stem composed of titanium alloy with a dual taper, rectangular, and trochanteric wing design. (c) Accolade TMZF stem (Stryker Orthopaedics, Mahwah, NJ) is a cementless tapered wedge-type stem composed of beta titanium alloy with a proximal hydroxyapatite-coated porous surface and a distal smooth-finished surface.

We investigated 24 patients (16 women and 8 men) who underwent primary cementless THA using the same fit-and-fill type of prosthesis (collarless VerSys Fiber Metal MidCoat, Zimmer Inc., Warsaw, IN) (**Figure 1**). Collarless VerSys Fiber Metal MidCoat is a stem composed of titanium alloy with a fiber-metal porous coating at the proximal region. Patients were excluded from the study if they were receiving systemic estrogen, vitamin D, or bisphosphonate for osteoporosis. The mean patient age at surgery was 63 years (range, 44–82 years). After surgery, all patients were allowed to use a wheelchair, with full weight bearing, on postoperative day 1, and gait exercise was performed as soon as possible [23]. BMD was assessed with dual-energy X-ray absorptiometry (DEXA) using the Hologic Discovery system (Hologic Inc., Waltham, MA). Baseline DEXA measurements were performed 1 week after surgery as reference, and subsequent measurements were performed at 3, 6, and 12 months postoperatively. Patients were placed in the supine position, and the affected leg was maintained in 20 ° internal rotation to minimize measurement errors. DEXA measurements were performed using the "array prosthetic" mode, which excludes metal from analysis of the regions of interest (ROIs). ROIs were defined according to Gruen's system [28]. The pixel size was 1.1 × 0.56 mm.

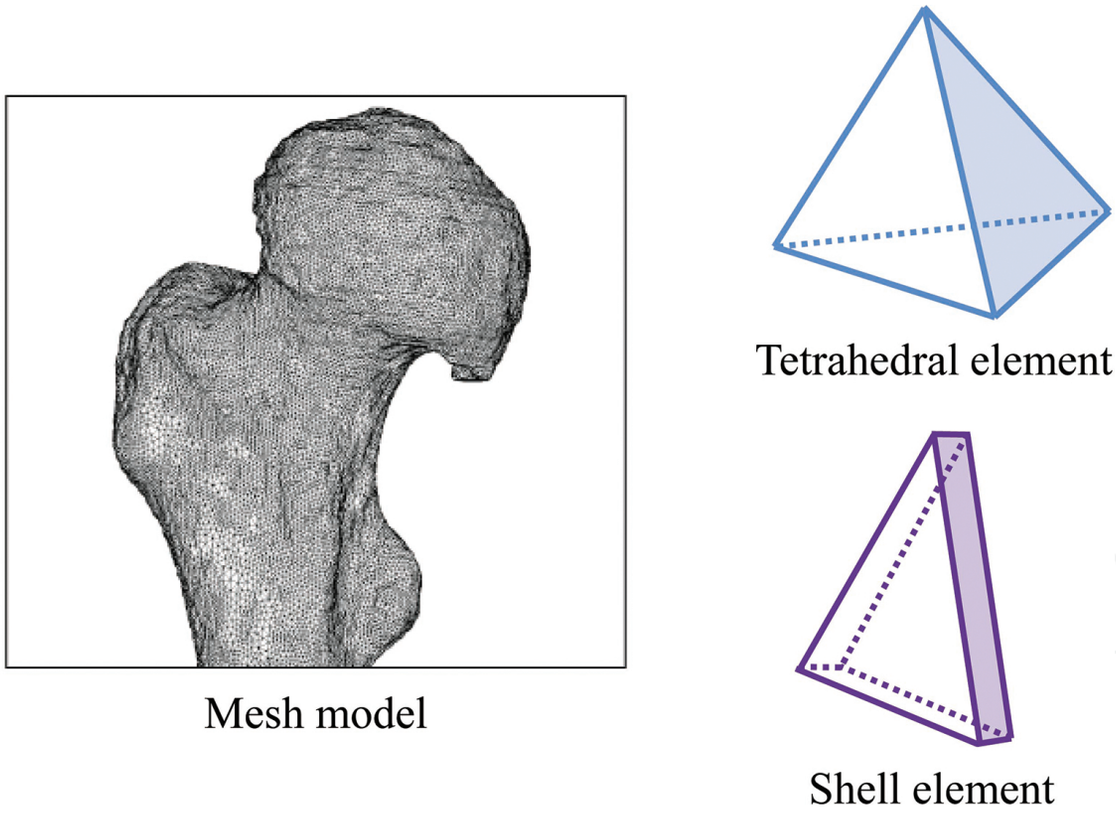

Figure 2. Finite element mesh of the femur. Three-dimensional FE models are constructed using 1- to 4-mm tetrahedral elements for the trabecular and inner cortical bone. The outer surface of the cortical bone is represented with three nodal-point shell elements having a thickness of 0.3 mm.

CT scans of the femurs of all patients were performed pre- and postoperatively (1 week after surgery). The scanner settings were approximately 140 kV and 300 mA, with a slice thickness

of 2 mm, pixel resolution of 512 × 512, and voxel size of 0.70 × 0.70 × 2 mm. Three-dimensional FE models of the femur and stem were constructed according to pre- and postoperative CT data using the Mechanical Finder ver. 6.0 software (Research Center of Computational Mechanics Inc., Tokyo, Japan). This software creates FE models after considering individual bone shape and density distribution [29]. We used a global threshold algorithm for determining the bone area with a threshold of 200 mg/cm^3 and with manual correction if necessary. We applied a closing algorithm in addition to the global threshold algorithm for determining the bone area when the density was extremely low [29]. In addition, the global threshold algorithm was applied to determine the stem area with a threshold of 2,000 Hounsfield units. We used 1 to 4 mm tetrahedral elements to construct three-dimensional FE models for the trabecular and inner cortical bone. The outer surface of the cortical bone was represented with three nodal-point shell elements having a thickness of 0.3 mm (**Figure 2**). The FE models of the femur consisted of approximately 600,000 elements in addition to 200,000 elements for the stem. Bone density was determined according to CT density values, using a calibration equation (**Table 1**). Additionally, the elastic modulus of the bone was determined according to bone density values, using the equations proposed by Keyak et al. [18, 30] and Keller [31] (**Table 1**). Poisson's ratio of the bone was assumed to be 0.40. The stem was an isotropic titanium alloy, and it had an elastic modulus of 109.0 GPa and a Poisson's ratio of 0.28. The models assumed a completely bonded interface between the stem and bone. The models were restrained at the distal end of the femoral shaft, and loads were applied to the femoral head and greater trochanter. We applied a load of 2400 N to the surface of the femoral head at an angle of 15° to the femoral axis and applied a load of 1200 N to the greater trochanter at an angle of 20° [32, 33]. Linear FEA was performed. Equivalent stress and SED were analyzed in ROIs 1–7 and were compared with the DEXA data.

Bone density	Elastic modulus (MPa)
$\rho = 0$	0.001
$0 < \rho \leq 0.27$	$33{,}900\rho^{2.20}$
$0.27 < \rho < 0.6$	$5307\rho + 469$
$0.6 \leq \rho$	$10{,}200\rho^{2.01}$

$$\rho\left(\mathrm{g}/\mathrm{cm}^3\right) = (\mathrm{H.U.} + 1.4246) \times 0.001 \Big/ 1.508 \ (\mathrm{H.U.} > -1)$$
$$= 0.0 \ (\mathrm{H.U.} \leq -1)$$

H.U. represents CT density values in Hounsfield Units. The elastic modulus of the bone is determined according to computed tomography density values, using the equations proposed by Keyak et al. [18, 30] and Keller [31].

Table 1. Equations used for calculating the elastic modulus of the bone.

Changes in the BMD of the femur during the first postoperative year are shown in **Figure 3**. BMD was maintained in ROIs 3, 4, 5, and 6, whereas it significantly decreased in ROIs 1, 2, and 7 by 19, 11, and 27%, respectively, 12 months after THA. The changes in BMD noted in this study were similar to those reported in other studies [34, 35].

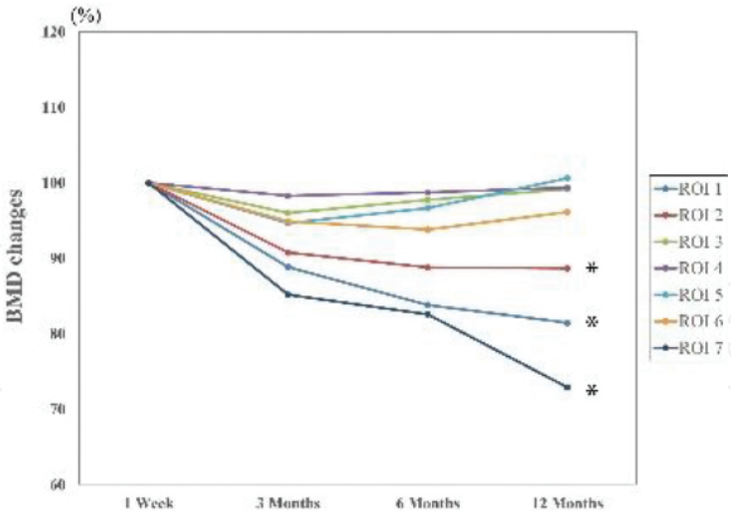

Figure 3. The median percentage change in bone mineral density (BMD) after surgery with the fit-and-fill-type stem. The periprosthetic BMDs at 3, 6, and 12 months after total hip arthroplasty (THA) are expressed as percentage changes from the baseline BMD measured at 1 week after surgery. BMD is maintained 12 months after THA in regions of interest (ROIs) 3, 4, 5, and 6, whereas it has significantly decreased by 19, 11, and 27% in ROIs 1, 2, and 7, respectively, 12 months after THA (*p< 0.05).

The pre- and postoperative equivalent stress and SED are shown in **Figure 4**. The equivalent stress and SED were maintained in ROIs 3, 4, and 5, whereas both decreased in ROIs 1, 2, 6, and 7 after THA (**Figure 5**). The lowest values of equivalent stress, SED, and relative BMD were observed in ROI 7 ($p < 0.05$). There was a relatively strong correlation between equivalent stress and BMD changes ($R = 0.426$, $p < 0.01$), whereas there was a weak correlation between SED and BMD changes ($R = 0.183$, $p = 0.053$) (**Figure 6**).

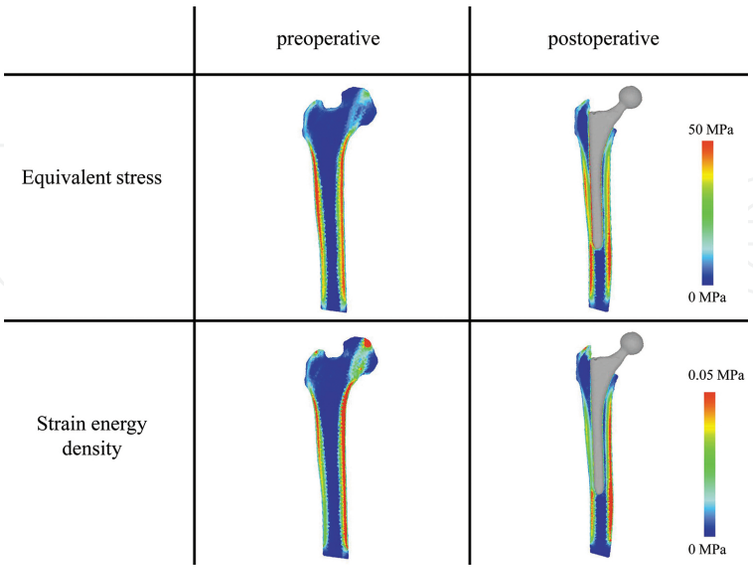

Figure 4. Distributions of equivalent stress and strain energy density (SED) in the femur. Equivalent stress and SED are maintained in the distal femur after total hip arthroplasty, whereas both decreased in the proximal femur.

http://dx.doi.org/10.5772/65031

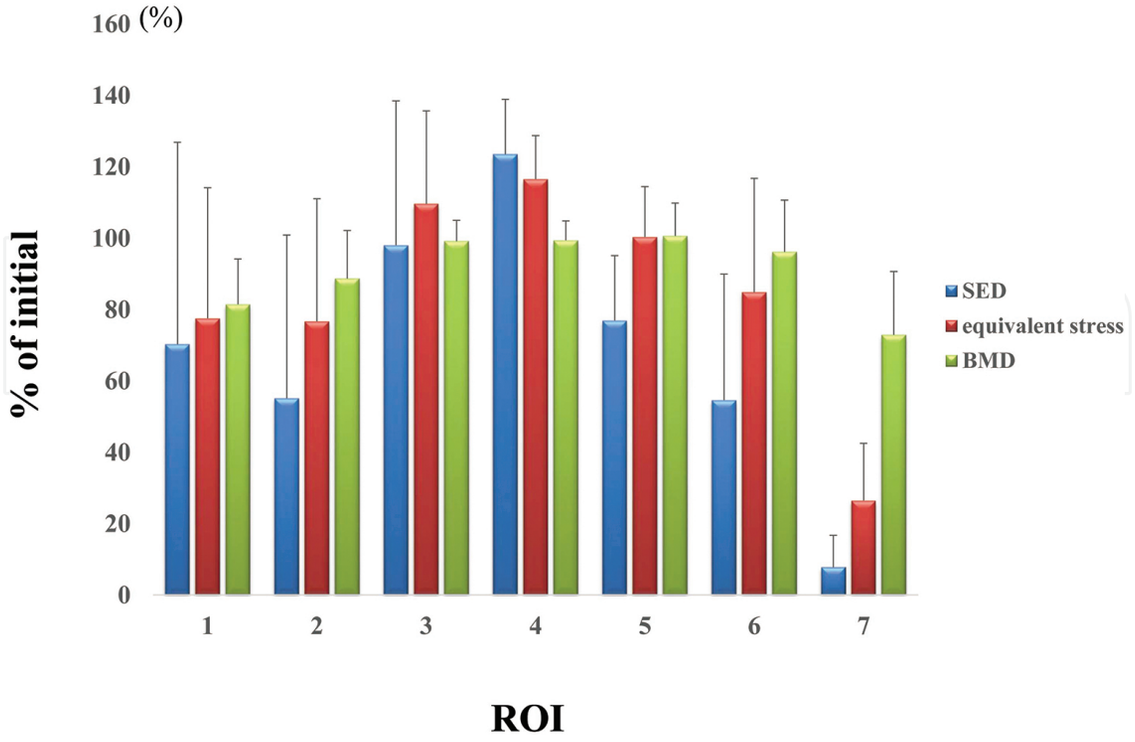

Figure 5. Strain energy density (SED), equivalent stress, and bone mineral density (BMD) 12 months after total hip arthroplasty. In ROI 7, equivalent stress, SED, and relative BMD show the lowest values of all regions examined.

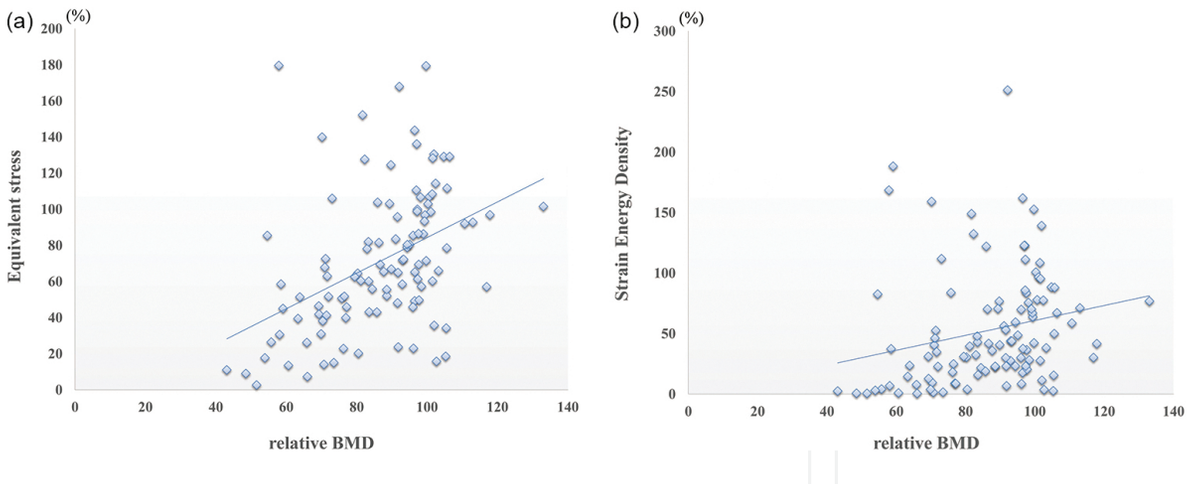

Figure 6. Scatter plots of the relationships (a) between bone mineral density (BMD) and equivalent stress and (b) between BMD and strain energy density (SED). The periprosthetic BMD at 12 months after total hip arthroplasty (THA) is expressed as the percentage change from the baseline BMD measured at 1 week after surgery. Postoperative equivalent stress and SED are expressed as percentage changes from the preoperative values. (a) Equivalent stress has a relatively strong correlation with the changes in BMD ($R = 0.426$, $p < 0.01$). (b) SED has a weak correlation with the changes in BMD ($R = 0.183$, $p = 0.053$).

Periprosthetic BMD loss may be related to changes in the mechanical loading environment. The purpose of this study was to investigate the relationships between periprosthetic BMD loss and changes in the mechanical loading environment after cementless THA according to

subject-specific FEA. This subject-specific FEA exhibited a significant correlation between BMD changes and equivalent stress. After THA, the stress load is transferred to the distal femur through the stem rather than to the periprosthetic bone owing to the high elastic modulus of the stem [36, 37]. Therefore, equivalent stress in the proximal femur may decrease after stem implantation. These results are consistent with those of previous studies [20, 33]. We investigated the effect of a porous-coated titanium-alloy fit-and-fill-type stem on bone remodeling after THA. Although this implant is designed to achieve proximal fixation, equivalent stress and BMD decreased postoperatively at the proximal femur. These results indicate that load transmission to the proximal femur may not be sufficient for maintaining BMD.

The present study demonstrated that equivalent stress correlates with BMD changes in the femur 12 months after THA. In this study, CT scans were performed from all patients pre- and postoperatively, and subject-specific FE models were constructed to investigate bone heterogeneity by using the equations proposed by Keyak et al. [18, 30] and Keller [31]. Our results suggest that the rate of changes in equivalent stress could be an important factor for BMD changes.

The strain-adaptive bone-remodeling theory has been used to simulate BMD changes after THA; Huiskes et al. [14] reported that the SED distribution indicates the regions where resorption and apposition are expected. However, other studies have reported that bone remodeling can be better predicted with stress parameters than with strain parameters. Simulation results and clinical data have shown that there is a positive correlation between average equivalent stress and BMD [38, 39]. Therefore, controversy still exists with regard to whether equivalent stress or SED is an appropriate parameter for evaluating bone remodeling. Our results suggest that a decrease in equivalent stress caused a decrease in BMD in the proximal femur after THA.

2.2. Effects of stem geometry

A number of factors, such as geometry, roughness and coating of the stem, technique of preparation, and bone quality, influence initial stability or primary fixation. Femoral stems with various geometries are currently in use. The implant shape has been shown to determine cortical contact and initial stability [40]. Our recent study showed that differences in stem design could affect the postoperative BMD loss of the proximal femur [41]. We studied the effects of stem geometry on BMD changes and equivalent stress in the femur after THA.

We investigated 20 patients who underwent primary cementless THA for osteoarthritis or osteonecrosis of the hip. Of these patients, 10 underwent THA with a Zweymüller-type stem (SL-PLUS; Smith & Nephew Inc.), and the other 10 underwent THA with a fit-and-fill-type stem (collarless VerSys Fiber Metal MidCoat; Zimmer Inc.) (**Figure 1**). The mean age of the patients at the time of THA was 63 years (range, 54–72 years) in the Zweymüller-type stem group and 64 years (range, 57–69 years) in the fit-and-fill-type stem group. There was no significant difference in age between the two groups. In the Zweymüller-type stem group, all patients were diagnosed with osteoarthritis, while in the fit-and-fill-type stem group, eight patients were diagnosed with osteoarthritis, and two were diagnosed with osteonecrosis. We compared equivalent stress and BMD between the two groups.

http://dx.doi.org/10.5772/65031

In the preoperative models, no significant differences in equivalent stress were observed between the two groups. In the postoperative models, maximum equivalent stress was observed in ROI 4, and minimum equivalent stress was observed in ROI 1 in both groups. In ROI 4, equivalent stress was significantly higher in the Zweymüller-type stem group than in the fit-and-fill-type stem group ($p < 0.05$). On the other hand, in ROI 7, equivalent stress was significantly higher in the fit-and-fill-type stem group than in the Zweymüller-type stem group ($p < 0.05$) (**Figure 7**).

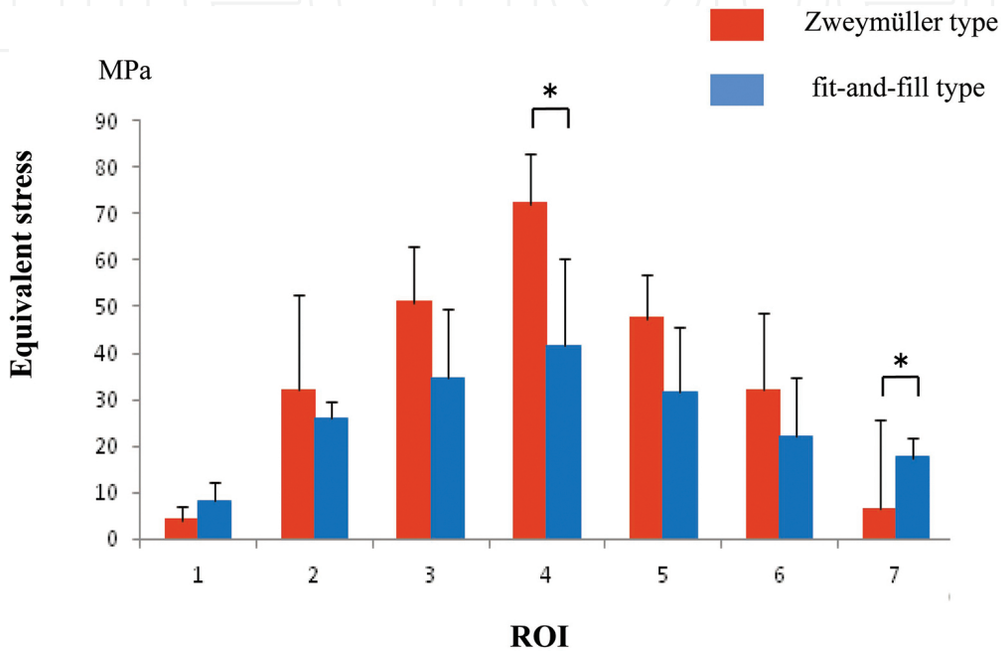

Figure 7. Comparison of equivalent stress between the fit-and-fill-type stem and Zweymüller-type stem groups. The equivalent stress in ROI 4 is higher, and the stress in ROI 7 is lower in the Zweymüller-type stem group than in the fit-and-fill-type stem group *$p< 0.05$.

Changes in the BMD of the femur during the first postoperative year are shown in **Figure 8**. In both the Zweymüller-type stem and fit-and-fill-type stem groups, BMD decreased in ROIs 2, 6, and 7, whereas BMD was maintained in ROIs 3, 4, and 5. In ROIs 6 and 7, BMD was significantly lower in the Zweymüller-type stem group than in the fit-and-fill-type stem group ($p < 0.05$). In ROI 1, the fit-and-fill-type stem group showed a continuous decrease in BMD for 12 months after surgery, while the Zweymüller-type stem group showed a decrease in BMD up to 6 months after surgery and then showed an increase 12 months after surgery. In ROI 4, BMD was significantly lower in the fit-and-fill-type stem group than in the Zweymüller-type stem group at 3 months after surgery ($p < 0.05$); however, there were no differences in BMD between the two groups at 6 months or 12 months after surgery [24].

Stress at the proximal femur was lower, and stress at the distal femur was higher in the Zweymüller-type stem group than in the fit-and-fill-type stem group. BMD at the proximal femur was significantly lower in the Zweymüller-type stem group than in the fit-and-fill-type stem group ($p < 0.05$). The FEA results and postoperative BMD changes in the femur suggest

that implantation of the Zweymüller-type stem leads to insufficient load transmission to the proximal femur and may be associated with proximal BMD loss. These findings indicate that subject-specific FEA can assess the effects of stem geometry on adaptive bone remodeling after THA.

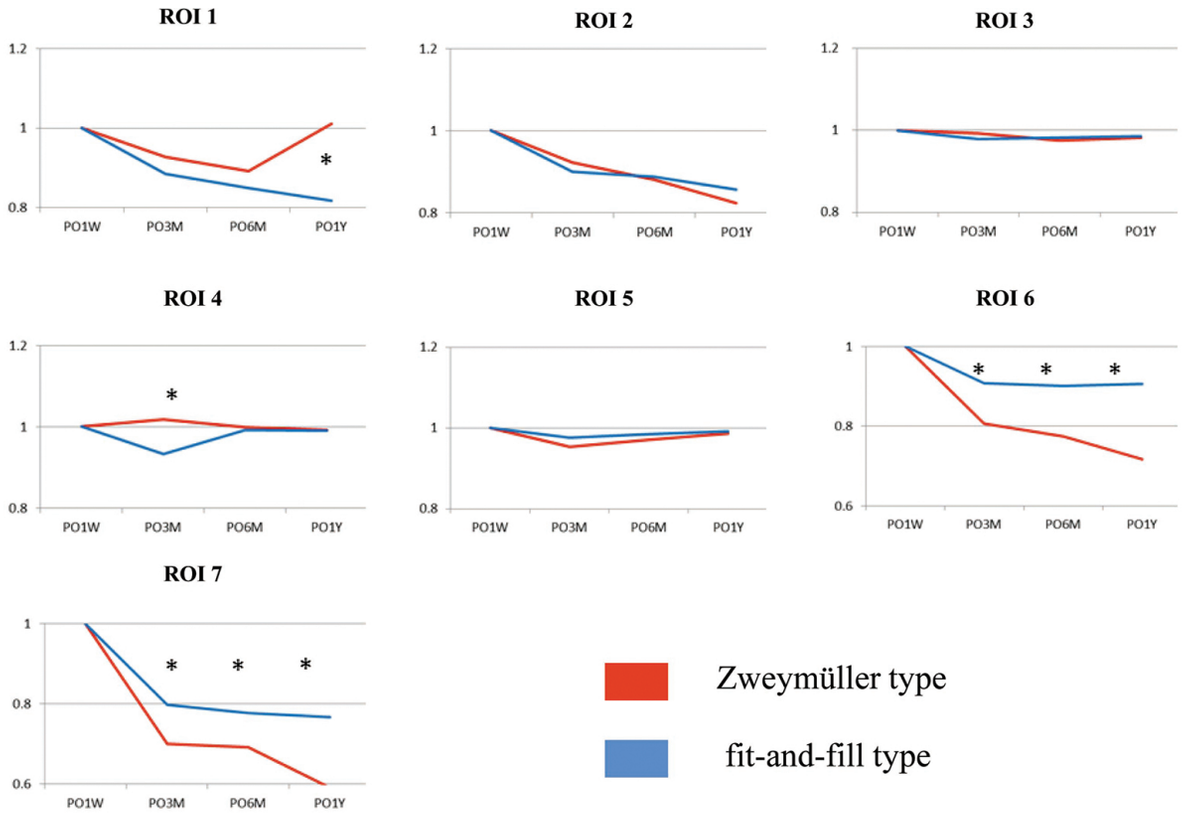

Figure 8. Median percentage change in bone mineral density (BMD) after surgery in the fit-and-fill-type stem and Zweymüller-type stem groups. The periprosthetic BMDs at 3, 6, and 12 months after surgery are expressed as percentage changes from the baseline BMD measured at 1 week after surgery (*$p < 0.05$).

2.3. Effects of bone geometry

Noble et al. [42] demonstrated the femoral anatomy variations in the mediolateral and anteroposterior dimensions and the need for multiple stem designs to achieve a close fit. Close adaptation of the prosthesis to the bone geometry is required to achieve optimal primary stability and secondary biologic fixation [43]. We studied the effects of bone geometry on BMD changes and equivalent stress in the femur after THA.

We investigated 20 patients who underwent THA using the Accolade TMZF stem (Stryker Orthopaedics) after reviewing the preoperative anterior-posterior hip radiographs of 90 consecutive patients who had undergone THA using the Accolade TMZF stem (**Figure 1**). The width of the proximal femoral canal on the operated side was measured from preoperative anterior-posterior hip radiographs, and Noble's canal flare index (CFI) was calculated for each patient [42]. Based on Noble's classification, the femurs were divided into the following three

http://dx.doi.org/10.5772/65031

groups of femoral canal shapes: champagne flute (CFI ≥ 4.7), intermediate (CFI 3–4.7), and stovepipe (CFI < 3). Among the 20 study femurs, 7 had a champagne flute canal shape, 5 had a stovepipe shape, and 8 had an intermediate canal shape. The 8 femurs with an intermediate canal shape were randomly selected from among the remaining 78 hips with an intermediate canal shape to balance the groups for analysis.

The mean percentage changes in equivalent stress in each ROI between the pre- and postoperative femur models were calculated from the FEA results, and they are plotted in **Figure 9**. Between-group differences in the pattern of postoperative changes in equivalent stress were identified, and specific differences were observed in ROIs 6 ($p = 0.01$) and 7 ($p = 0.02$). Post hoc analysis indicated that the decrease in equivalent stress in ROI 6 was significantly greater in the stovepipe group (−63.8%) than in the champagne flute group (−38.8%) and intermediate group (−47.2%) ($p = 0.01$). Additionally, the decrease in equivalent stress in ROI 7 was significantly greater in the stovepipe group (−70.9%) than in the champagne flute group (−53.7%) and intermediate group (−51.4%) ($p = 0.03$).

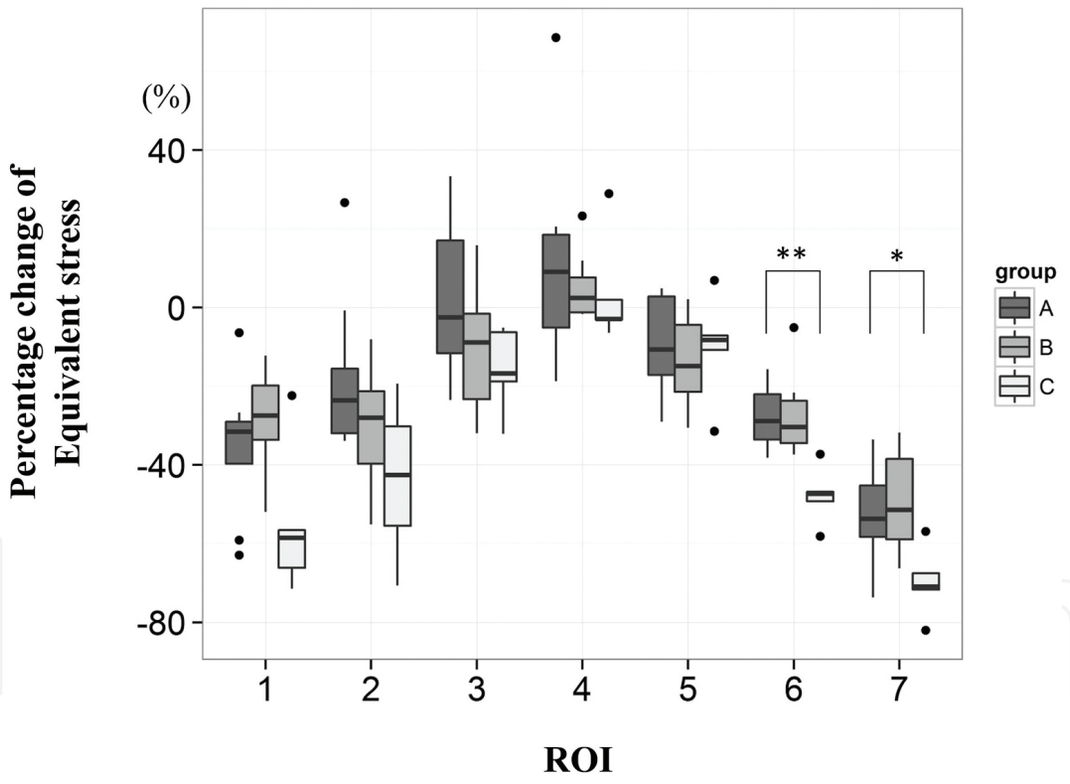

Figure 9. Comparison of the relative percentage changes in equivalent stress between the pre- and postoperative femur models for the three femoral canal shape groups. Postoperative relative percentage changes in equivalent stress in each region of interest compared to that of the preoperative models. Dots in the box plot show the outliers (*$p = 0.02$, **$p = 0.01$).

BMD changes in the femurs during the first postoperative year are shown in **Figure 10**. Significant between-group differences in BMD were evident in ROIs 6 ($p = 0.01$) and 7 ($p = 0.04$). In ROI 6, a marked decrease in BMD was identified only in the stovepipe group during the

first postoperative year; the ROI 6 BMD showed a significantly higher decrease in the stovepipe group (−14.3%) than in the champagne flute group (−1.4%) and intermediate group (+3.6%) (p = 0.01). A postoperative decrease in ROI 7 BMD was evident in all the groups during the first postoperative year (champagne flute group, −23.1%; intermediate group, −22.7%; and stovepipe group, −36.5%). Additionally, the ROI 7 BMD showed a significantly higher decrease in the stovepipe group than in the other two groups (p = 0.045). BMDs in ROIs 1 and 2 were relatively lower in the stovepipe group than in the champagne flute and stovepipe groups during the first postoperative year; however, the differences were not significant.

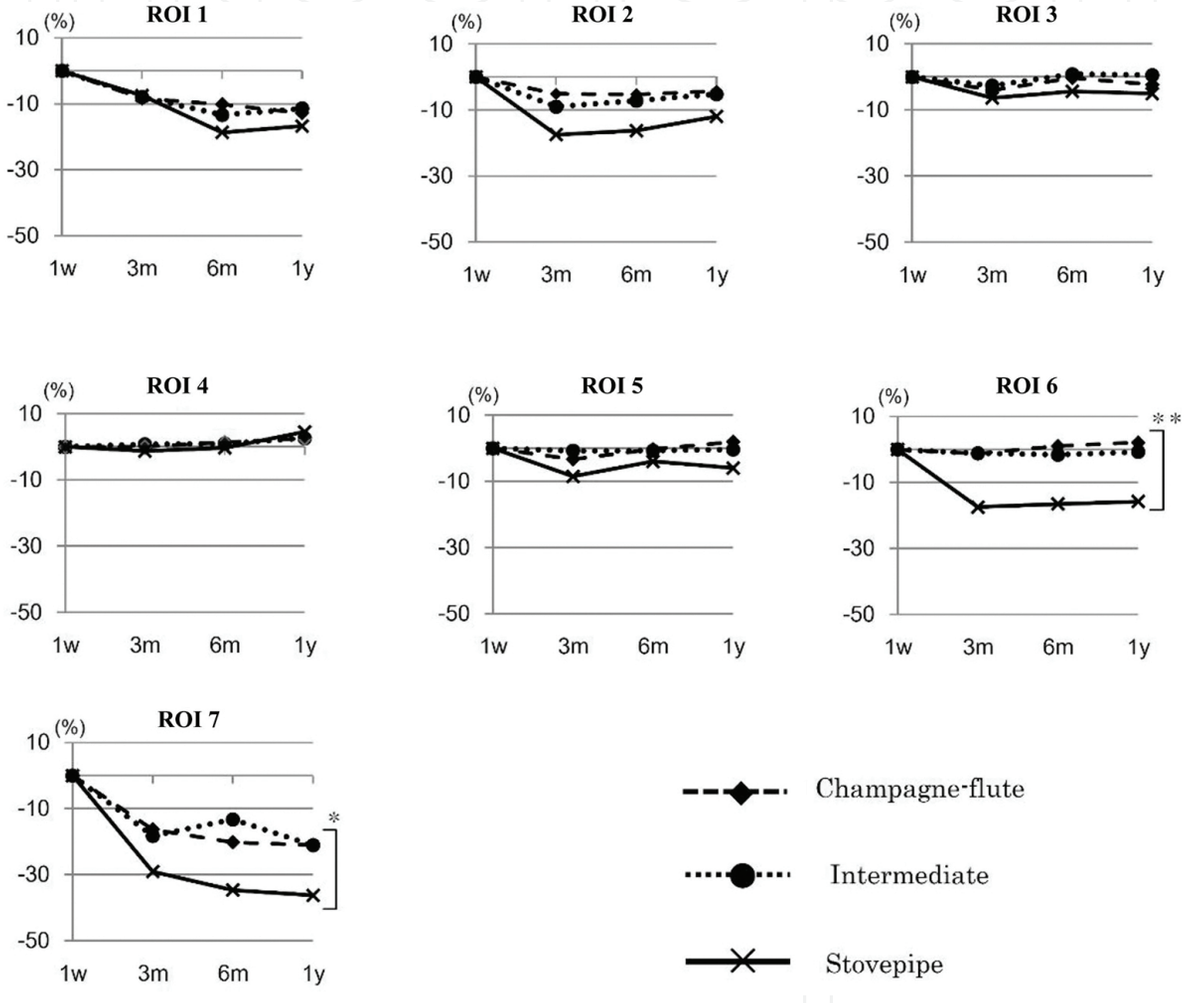

Figure 10. Comparison of bone mineral density (BMD) in the three femoral canal shape groups. The periprosthetic BMDs at 3, 6, and 12 months after surgery are expressed as percentage changes from the baseline BMD measured at 1 week after surgery (*p = 0.04, **p = 0.01).

The percentage changes in equivalent stress in each ROI were positively correlated with the postoperative BMD changes (**Figure 11**). A significant correlation was observed between equivalent stress and BMD changes (p < 0.01), and the adjusted R^2 value showed that the percentage changes in equivalent stress (adjusted R^2 = 0.79) could predict the postoperative BMD changes in our simulation model.

http://dx.doi.org/10.5772/65031

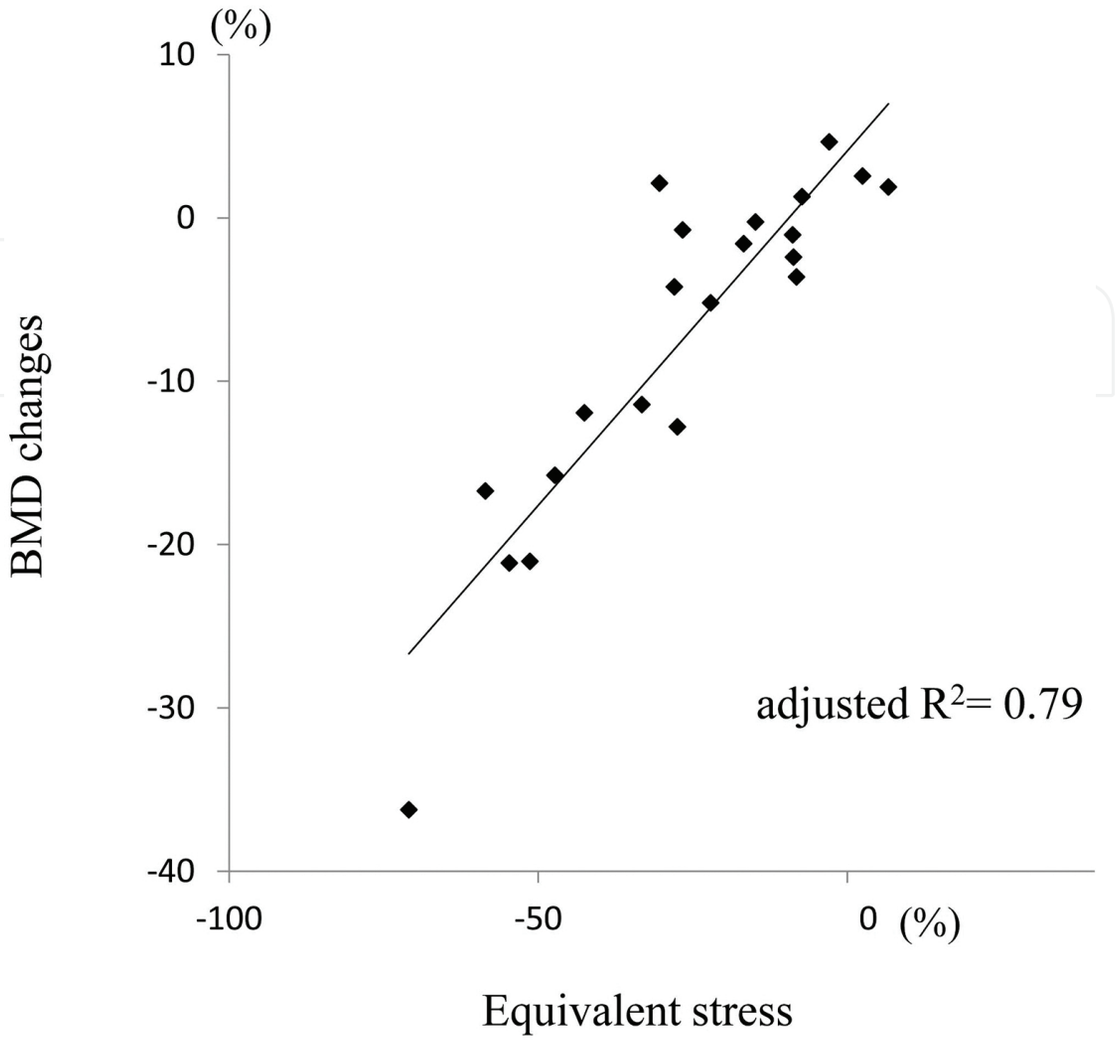

Figure 11. Scatter plot illustrating the relationship between the percentage changes in equivalent stress and postoperative bone mineral density (BMD). The 21 points plotted in this scatter plot display the average relative percentage changes in equivalent stress (finite element analysis results) and BMD for the three femoral canal shape groups. A significant correlation is observed between equivalent stress and BMD changes (adjusted $R^2 = 0.79$, $p < 0.01$).

The FEA results and postoperative BMD changes of the femur suggest that the combination of a large, tapered wedge-type stem and stovepipe femur may be associated with proximal BMD loss. Our simulation-based outcomes predicted a stronger stress-shielding effect in the stovepipe femur group than in the other groups. These results indicate that subject-specific FEA can assess the effects of bone geometry on adaptive bone remodeling after THA.

The present studies have limitations. First, the interface condition between the stem and the femur in the FEA model was assumed to be fully bonded. Consideration of the surface properties of the implant and degree of stem fixation would be useful for constructing realistic models. Second, the maximum length of the tetrahedral elements (4 mm) was relatively large, and therefore the elements might straddle the boundary between the cortical and cancellous area in the FE models. Therefore, the elastic modulus of the elements straddling the boundary would contain some errors.

3. Summary

We focused on equivalent stress as a mechanical parameter associated with adaptive bone remodeling and found that equivalent stress changes were positively correlated with postoperative BMD changes in the femur. BMD and equivalent stress were maintained in the distal femur and decreased in the proximal femur after THA. Thus, the proposed subject-specific FEA is useful for evaluating adaptive bone remodeling after THA and could predict BMD changes after THA. Furthermore, subject-specific FEA can be used to evaluate the effects of stem geometry and bone geometry on bone remodeling and can help in the understanding of the altered mechanical environment after THA.

Abbreviations

BMD, bone mineral density

CFI, canal flare index

CT, computed tomography

DEXA, dual-energy X-ray absorptiometry

FEA, finite element analysis

ROIs, regions of interest

SED, strain energy density

THA, total hip arthroplasty

Author details

Yutaka Inaba*, Hiroyuki Ike, Masatoshi Oba and Tomoyuki Saito

*Address all correspondence to: yute0131@med.yokohama-cu.ac.jp

Department of Orthopaedic Surgery, Yokohama City University, Yokohama, Japan

References

[1] Malchau H, Herberts P, Ahnfelt L. Prognosis of total hip replacement in Sweden. Follow-up of 92,675 operations performed 1978-1990. Acta Orthop Scand. 1993; 64:497–506.

[2] Dorr LD, Lewonowski K, Lucero M, Harris M, Wan Z. Failure mechanisms of anatomic porous replacement I cementless total hip replacement. Clin Orthop Relat Res. 1997; 334:157–167.

[3] Bougherara H, Bureau M, Campbell M, Vadean A, Yahia L. Design of a biomimetic polymer-composite hip prosthesis. J Biomed Mater Res. 2007; 82:27–40.

[4] Kerner J, Huiskes R, van Lenthe GH, Weinans H, van Rietbergen B, Engh CA, Amis AA. Correlation between pre-operative periprosthetic bone density and post-operative bone loss in THA can be explained by strain-adaptive remodelling. J Biomech. 1999; 32:695–703.

[5] Kroger H, Miettinen H, Arnala I, Koski E, Rushton N, Suomalainen O. Evaluation of periprosthetic bone using dual-energy X-ray absorptiometry: precision of the method and effect of operation on bone mineral density. J Bone Miner Res. 1996; 11:1526–1530.

[6] Kim YH, Yoon SH, Kim JS. Changes in the bone mineral density in the acetabulum and proximal femur after cementless total hip replacement: alumina-on-alumina versus alumina-on-polyethylene articulation. J Bone Joint Surg Br. 2007; 89:174–179.

[7] Nishii T, Sugano N, Masuhara K, Shibuya T, Ochi T, Tamura S. Longitudinal evaluation of time related bone remodeling after cementless total hip arthroplasty. Clin Orthop Relat Res. 1997; 339:121–131.

[8] Kroger H, Venesmaa P, Jurvelin J, Miettinen H, Suomalainen O, Alhava E. Bone density at the proximal femur after total hip arthroplasty. Clin Orthop Relat Res. 1998; 352:66–74.

[9] Rosenthall L, Bobyn JD, Brooks CE. Temporal changes of periprosthetic bone density in patients with a modular noncemented femoral prosthesis. J Arthroplasty. 1999; 14:71–76.

[10] Ostbyhaug PO, Klaksvik J, Romundstad P, Aamodt A. An in vitro study of the strain distribution in human femora with anatomical and customised femoral stems. J Bone Joint Surg Br. 2009; 91:676–682.

[11] Wolff J. Das Gesetz der Transformation der Knochen. Berlin, Germany: Verlag von August Hirschwald; 1892.

[12] Jaworski ZF. Coupling of bone formation to bone resorption: a broader view. Calcif Tissue Int. 1984; 36:531–535.

[13] Zadpoor AA. Open forward and inverse problems in theoretical modeling of bone tissue adaptation. J Mech Behav Biomed Mater. 2013; 27:249–261.

[14] Huiskes R, Weinans H, Grootenboer HJ, Dalstra M, Fudala B, Slooff TJ. Adaptive bone-remodeling theory applied to prosthetic-design analysis. J Biomech. 1987; 20:1135–1150.

[15] Carter DR, Van Der Meulen MC, Beaupre GS. Mechanical factors in bone growth and development. Bone. 1996; 18:5S–10S.

[16] Stulpner MA, Reddy BD, Starke GR, Spirakis A. A three-dimensional finite analysis of adaptive remodelling in the proximal femur. J Biomech. 1997; 30:1063–1066.

[17] Adachi T, Tomita Y, Sakaue H, Tanaka M. Simulation of trabecular surface remodeling based on local stress uniformity. Jpn Soc Mech Eng. 1997; 40:782–792.

[18] Keyak JH, Rossi SA, Jones KA, Skinner HB. Prediction of femoral fracture load using automated finite element modeling. J Biomech. 1998; 31:125–133.

[19] Taddei F, Schileo E, Helgason B, Cristofolini L, Viceconti M. The material mapping strategy influences the accuracy of CT-based finite element models of bones: an evaluation against experimental measurements. Med Eng Phys. 2007; 29:973–979.

[20] Pettersen SH, Wik TS, Skallerud B. Subject specific finite element analysis of stress shielding around a cementless femoral stem. Clin Biomech (Bristol, Avon). 2009; 24:196–202.

[21] Cody DD, Gross GJ, Hou FJ, Spencer HJ, Goldstein SA, Fyhrie DP. Femoral strength is better predicted by finite element models than QCT and DXA. J Biomech. 1999; 32:1013–1020.

[22] Tawara D, Sakamoto J, Murakami H, Kawahara N, Oda J, Tomita K. Mechanical evaluation by patient-specific finite element analyses demonstrates therapeutic effects for osteoporotic vertebrae. J Mech Behav Biomed Mater. 2010; 3:31–40.

[23] Ike H, Inaba Y, Kobayashi N, Hirata Y, Yukizawa Y, Aoki C, Choe H, Saito T. Comparison between mechanical stress and bone mineral density in the femur after total hip arthroplasty by using subject-specific finite element analyses. Comput Methods Biomech Biomed Engin. 2015; 18:1056–1065.

[24] Hirata Y, Inaba Y, Kobayashi N, Ike H, Fujimaki H, Saito T. Comparison of mechanical stress and change in bone mineral density between two types of femoral implant using finite element analysis. J Arthroplasty. 2013; 28:1731–1735.

[25] Anderson AE, Peters CL, Tuttle BD, Weiss JA. Subject-specific finite element model of the pelvis: development, validation and sensitivity studies. J Biomech Eng. 2005; 127:364–373.

[26] Ateshian GA, Henak CR, Weiss JA. Toward patient-specific articular contact mechanics. J Biomech. 2015; 48:779–786.

[27] Weinans H, Sumner DR, Igloria R, Natarajan RN. Sensitivity of periprosthetic stress-shielding to load and the bone density-modulus relationship in subject-specific finite element models. J Biomech. 2000; 33:809–817.

[28] Gruen TA, McNeice GM, Amstutz HC. "Modes of failure" of cemented stem-type femoral components: a radiographic analysis of loosening. Clin Orthop Relat Res. 1979; 141:17–27.

[29] Bessho M, Ohnishi I, Matsuyama J, Matsumoto T, Imai K, Nakamura K. Prediction of strength and strain of the proximal femur by a CT-based finite element method. J Biomech. 2007; 40:1745–1753.

[30] Keyak JH, Lee IY, Skinner HB. Correlations between orthogonal mechanical properties and density of trabecular bone: use of different densitometric measures. J Biomed Mater Res. 1994; 28:1329–1336.

[31] Keller TS. Predicting the compressive mechanical behavior of bone. J Biomech. 1994; 27:1159–1168.

[32] Bergmann G, Deuretzbacher G, Heller M, Graichen F, Rohlmann A, Strauss J, Duda GN. Hip contact forces and gait patterns from routine activities. J Biomech. 2001; 34:859–871.

[33] Herrera A, Panisello JJ, Ibarz E, Cegonino J, Puertolas JA, Gracia L. Comparison between DEXA and finite element studies in the long-term bone remodeling of an anatomical femoral stem. J Biomech Eng. 2009; 131:041013.

[34] Aldinger PR, Sabo D, Pritsch M, Thomsen M, Mau H, Ewerbeck V, Breusch SJ. Pattern of periprosthetic bone remodeling around stable uncemented tapered hip stems: a prospective 84-month follow-up study and a median 156-month cross-sectional study with DXA. Calcif Tissue Int. 2003; 73:115–121.

[35] Boden H, Adolphson P. No adverse effects of early weight bearing after uncemented total hip arthroplasty: a randomized study of 20 patients. Acta Orthop Scand. 2004; 75:21–29.

[36] Maistrelli GL, Fornasier V, Binnington A, McKenzie K, Sessa V, Harrington I. Effect of stem modulus in a total hip arthroplasty model. J Bone Joint Surg Br. 1991; 73:43–46.

[37] Decking R, Puhl W, Simon U, Claes LE. Changes in strain distribution of loaded proximal femora caused by different types of cementless femoral stems. Clin Biomech (Bristol, Avon). 2006; 21:495–501.

[38] Herrera A, Panisello JJ, Ibarz E, Cegonino J, Puertolas JA, Gracia L. Long-term study of bone remodelling after femoral stem: a comparison between dexa and finite element simulation. J Biomech. 2007; 40:3615–3625.

[39] Kwon JY, Naito H, Matsumoto T, Tanaka M. Estimation of change of bone structures after total hip replacement using bone remodeling simulation. Clin Biomech (Bristol, Avon). 2013; 28:514–518.

[40] Khanuja HS, Vakil JJ, Goddard MS, Mont MA. Cementless femoral fixation in total hip arthroplasty. J Bone Joint Surg Am. 2011; 93:500–509.

[41] Inaba Y, Kobayashi N, Oba M, Ike H, Kubota S, Saito T. Difference in postoperative periprosthetic bone mineral density changes between 3 major designs of uncemented stems: a 3-year follow-up study. J Arthroplasty. DOI: 10.1016/j.arth.2016.02.009.

[42] Noble PC, Alexander JW, Lindahl LJ, Yew DT, Granberry WM, Tullos HS. The anatomic basis of femoral component design. Clin Orthop Relat Res. 1988; 235:148–165.

[43] Massin P, Geais L, Astoin E, Simondi M, Lavaste F. The anatomic basis for the concept of lateralized femoral stems: a frontal plane radiographic study of the proximal femur. J Arthroplasty. 2000; 15:93–101.

IntechOpen